Further investigations on ToF cameras distance errors and their corrections.

D. Falie, V. Buzuloiu
The Image Processing and Analysis Laboratory, Polytechnic University of Bucharest, Romania
dfalie@alpha.imag.pub.ro , buzuloiu@alpha.imag.pub.ro

***Abstract*—The distance calibration of the Time of Flight camera is a difficult task due to the errors produced by multi reflections of the light inside the camera body and outside. In any room the active light emitted by the camera is reflected by the walls and the objects in the scene. Thus the reflected light by the objects in the scene is the sum of this light and the direct light emitted by the camera. The distance information is affected by this indirect light.**

The calibration method we propose can be performed not only in laboratory condition but also in any conditions. The distance errors for all objects in the scene can be corrected if white or black tags (labels) are attached on objects.

I. Introduction

The ToF cameras -- type of 3D cameras dedicated to various applications where an image of the distances to the objects in the scene is the essential new ingredient -- are succinctly described in [4], [5], [6] and in our companion paper [3] of this conference and we invite the interested reader to refer to it for the description of the work principle of the ToF cameras. Here we just mention that, at this stage of the technology, the distance measurements are affected by very important errors due to multiple reflections of the direct light on external objects as well as inside the camera and that a main task towards the improvement of these cameras is to analyze this perturbing component of the "active" light arriving on a pixel and to find methods to compensate it. These cameras have their own source of light which is an infrared radiation (produced by an array of LED's) amplitude modulated with 20 MHz, which is reflected by the objects in the scene and then detected by each pixel detector, as an amplitude and phase (compared to the emitted 20 MHz wave). So, each pixel i will output at a given instant a complex signal,

$$I_m(i) = a_m(i) \cdot e^{j \cdot \varphi_m(i)} \tag{1}$$

where index m stands for "measured". If the only component of the incoming light would be for the point in the scene corresponding to the pixel in the image:

$$I_d(i) = a_d(i) \cdot e^{j \cdot \varphi_d(i)} \tag{2}$$

the phase φ(i) would be in a direct and simple relation to the distance of that point of the scene to the camera [4]

$$2 \cdot d(i) = \frac{c}{2 \cdot \pi \cdot f} \cdot \varphi(i) \tag{3}$$

where c is the speed of light and f is the modulation frequency (see also Fig. 1).

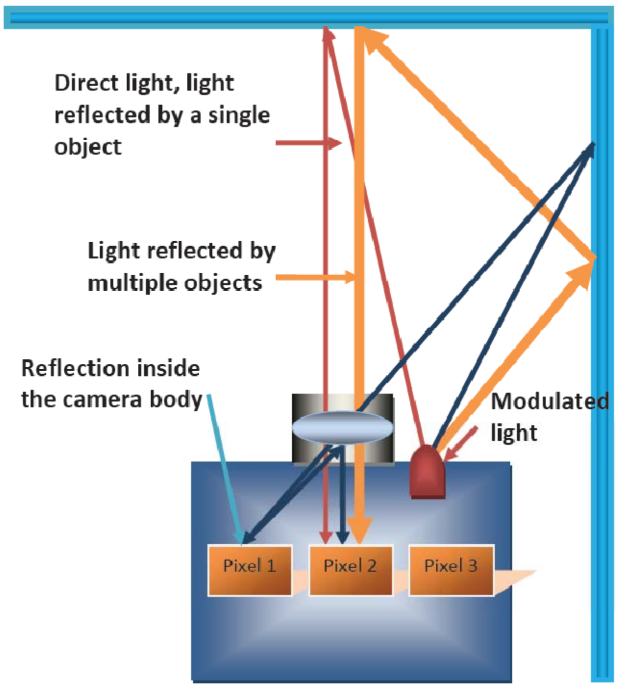

Figure 1. The object in the scene is iluminated directly by the modulated light and indirectly by the light reflected by other objects. Inside the camera body the incoming light is reflected by the chip surface to the lenses surface and back to the chip.

In any real setting the incoming light has many other components but only those coming from our "active source" will influence the output of the pixel detector; unfortunately there are such parasite components produced by multiple reflections (of the light from an active source) on various objects in the scene as well as by multiple reflections inside the camera. We denote these two kinds of parasite components by

$$I_{r1}(i) = a_{r1}(i) \cdot e^{j \cdot \varphi_{r1}(i)} \tag{4}$$

and

$$I_{r2}(i) = a_{r2}(i) \cdot e^{j \cdot \varphi_{r2}(i)} \tag{5}$$

and we shall put

$$I_p(i) = I_{r1}(i) + I_{r2}(i) = a_p(i) \cdot e^{j \cdot \varphi_p(i)} \tag{6}$$

sush that

$$I_m(i) = I_d(i) + I_p(i) \tag{7}$$

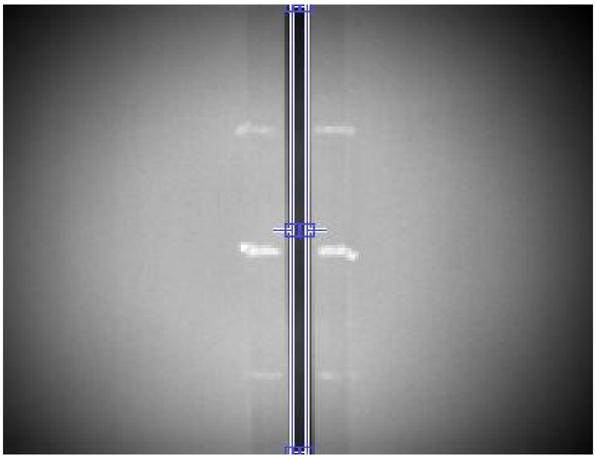

Figure 2. The Experimental setup: a black strip is painted on a white screen.

II. EXPERIMENTAL SETUP

To study the perturbation components above mentioned we have to use very simple images and we propose a vertical black strip on a white wall (Fig. 2) orthogonal on the line of sight, which is then displaced at various distances from the camera. For each setting we have two images: one is the amplitude image and the second one is the distance image. We select two neighbor vertical lines, one completely contained in the black strip and the other in the white region; i.e. one only having black points and the other only white points (in our experimental setup the distance between these two lines in the image was of 3 pixels). Now, as the wall is in a vertical plane orthogonal to the line of sight, the distance will vary symmetrically up and down and the curves of measured distances resulted for the two lines (black and white) are drawn in Fig. 3. It is obvious that in the center of the image the measured distance to the black line is bigger than that to the white line while up and down the difference is reversed; moreover, the two curves intersect each other in two (quasi-) symmetric points.

III. DISTANCE ERRORS CORRECTION.

Let consider the neighbor pixels (points) on the two lines, so one black and one white. We shall rewrite the relations (7) for these two points

$$I_m(i_1) = I_d(i_1) + I_p(i_1) \tag{8}$$

$$I_m(i_2) = I_d(i_2) + I_p(i_2) \tag{9}$$

The two pixels being neighbors it is obvious that the perturbation must be approximately the same and we shall admit that:

$$I_p(i_1) = I_p(i_2) \tag{10}$$

As the two pixels are neighbors, also their distances are the same and so their phases:

$$\varphi_d(i_1) = \varphi_d(i_2) \tag{11}$$

Only the amplitudes differ (we suppose the pixel i_1 is the black one):

$$a_d(i_1) \ll a_d(i_2) \tag{12}$$

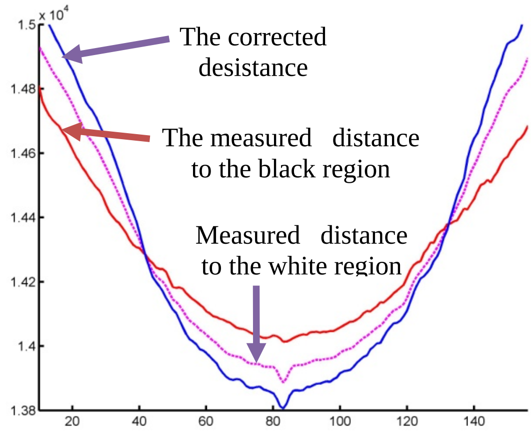

Figure 3. Plot of the measured distances along the blach and white vertical lines.

The diagrams of our vectors in the complex plane are drawn in Fig. 4 for smaller distances (smaller phase) as in the middle of the screen and for bigger distances (bigger phases) as near the border of the screen (noted with primes). We point out that the phase of the perturbation component is bigger than the phase φ_d because the distance of reflection path is generally higher for short distances of the object; and can become smaller for long distances (where φ_d is larger but the amplitude a_d becomes smaller). In our picture we used the same vector I_p for the two situations: pixels near the center of the image and pixels near the border of the image. Obviously this is only done for simplifying the drawing. Generally speaking, I_p will be different when changing the couple of pixels.

What is to stress here is that this diagram (Fig. 4, Fig. 5) is able to explain why the measurements for the black pixels are bigger in the center of the image and smaller near the border.

Even more important conclusion of this analysis of the vector diagram is that one can correct the measurement of the distance by comparing the values of the black and white neighboring pixels. Indeed, from equations (8)-(10) we infer that:

$$\Delta_m = I_m(i_2) - I_m(i_1) = I_d(i_2) - I_d(i_1) \tag{11}$$

and further

$$\Delta_m = (a_d(i_2) - a_{r2}(i_1)) \cdot e^{j \cdot \varphi_d(i_1)} \tag{12}$$

i.e. the phase of Δ_m will give the true distance because it has the true φ_d.

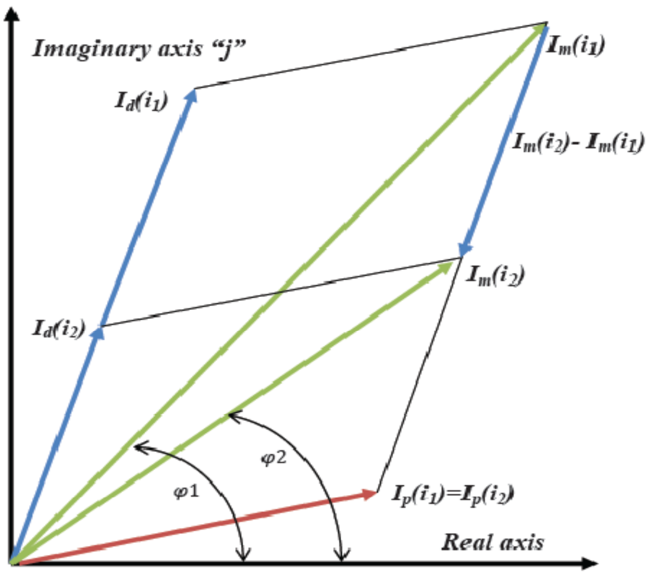

Figure 4. The graphical representation of the measured signals $I_m(i_1)$, $I_m(i_1)$, I_p and $I_m(i_2) - I_m(i_1) = I_d(i_2) - I_d(i_1)$.

Hence the method of drawing the corrected curve for distance in Fig. 3. The big advantage of this method is that it can be used in any real scene, just using white/black labels on the objects one wants to precisely measure their distances.

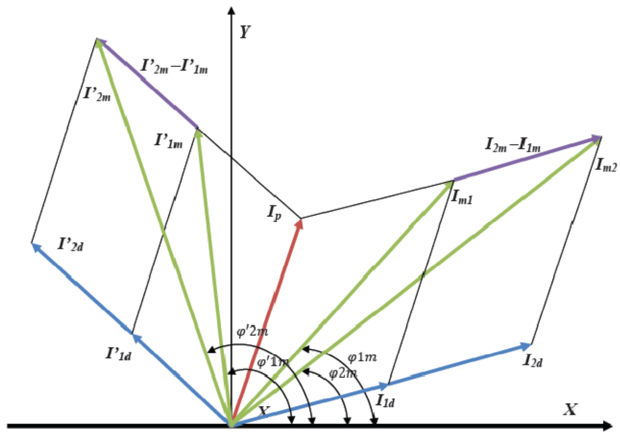

Figure 5. The graphical representation of the measured signals I_{1m} and I_{2m}, the perturbation signal I_p and the unperturbed signals I_{1d} and I_{2d}. With primes are represented the same signals at the edge of the picture.

IV. The Calibration of the Time of Flight Camera.

It is obvious from the above analysis that the calibration of a ToF camera for the distance measurements is a very complex task: Fig. 3 proves that neither white, nor black objects are appropriate for giving the real distance and this cannot obtained by any averaging (weighted or not) of these two distances (black and white).

Nevertheless, using a black/white pattern like in our setting, one can get the corrected value of the distance of a point (of a small region) of the scene from the vector diagram (Fig. 4 and eq. (12)). Such a correction can be made on many points of the image and so a rough calibration of the entire scene is obtained. We stress the fact that the vectorial model we proposed and any calibration method derived from it will give better results than any laboratory calibrations of the ToF camera which, in principle, are only valid for that particular laboratory scene.

From Fig. 3 one can also infer that there are points in the scene for which the “black” and “white” distances are equal (the same) and also the common value coincide with the real value so they could be ideal for calibration. Nevertheless from a practical point of view this is not very important because, in fact, the ideal calibration of a ToF camera would be a point wise (pixel wise) calibration depending of the scene.

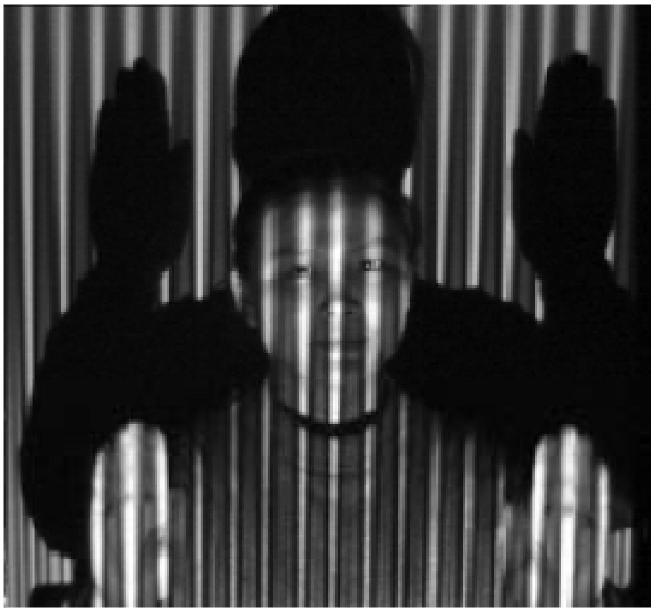

Figure 6. Example of an image taken with structured light [7].

For many industrial applications where the protective measures against infrared and laser light entering the human eyes are not necessary, a simple and reliable solution for a quasi pixel wise camera calibration will be the use of the so called structured light [7]: e.g. a small laser diode modulated with the same wave as the LED array and pointing to the object of interest from the scene, in two consecutive frames will get the same point once black, once white and with practically the same perturbing components. It is enough to have in these two frames a difference of the intensities

$$|a_m(i) - a_{m+1}(i)| > t_{\mathrm{a}},$$

where t_a is a threshold value, for being able to get the true value of the distance from the phase $\varphi_{\delta m}(i)$ of the difference

$$I_m(i) - I_{m+1}(i) = a_{\delta m}(i) \cdot e^{j \cdot \varphi_{\delta m}(i)}$$

V. Conclusion.

We have developed a vector model for the ToF camera measurements which allows us to explain a very important part of the distance errors in the distance images and also to propose methods for their correction in natural scenes. We also concluded that laboratory methods (i.e. with special scenes) for ToF camera calibration don't hold and live corrections/ calibration must be done for each scene independently. One suggestion is to use "labels" on the objects, another is to use structured light. A third will be developed in the future. But essential till now is the fact that the correction of the measured values by our method is able to drastically reduce the big distance errors observed on nowadays ToF cameras.

Acknowledgment

The ARTTS project is funded by the European Commission (contract no. IST-34107) within the Information Society Technologies (IST) priority of the 6th Framework Program.

This publication only reflects the views of the authors, and the Commission cannot be held responsible for any use which may be made of the information contained therein.

References

[1] D. Falie, V. Buzuloiu. Noise characteristics of 3D time-of-flight cameras, ISSCS, 2007, Iasi.

[2] S. Oprisescu, D. Falie, Mihai Ciuc, Vasile Buzuloiu, Measurements with ToF Cameras and their necessary corrections,ISSCS, 2007, Iasi.

[3] D. Falie and V. Buzuloiu, "Distance errors correction for the Time of Flight (ToF) Cameras," ECCSC '08.

[4] T. Oggier, M. Lehmann, R. Kaufmannn, M. Schweizer, M. Richter, P. Metzler, G. Lang, F. Lustenberger, N. Blanc, An all-solid-state optical range camera for 3D-real-time imaging with sub-centimeter depth-resolution (SwissRanger), Proc. SPIE Vol. 5249, pp. 634-545, 2003.

[5] T. Oggier, R. Kaufmann, M. Lehmann, P. Metzler, G. Lang, M. Schweizer, M. Richter, B. Büttgen, N. Blanc, K. Griesbach, B Uhlmann, K.-H. Stegemann, C. Ellmers, "3D-Imaging in Real-Time with Miniaturized Optical Range Camera", Opto Conference Nurnberg, 2004.

[6] T. Oggier, B. Büttgen, F. Lustenberger, "SwissRanger 3000 and first experiences based on miniaturized 3D- TOF camera", RIM Days, ETH Zurich, 2005.

[7] C. Guan, L. Hassebrook, and D. Lau, "Composite structured light pattern for three-dimensional video," Opt. Express **11**, 406-417 (2003)